Some novel nonlinear coherent excitations of the Davey–Stewartson system



2005 J. Phys. A: Math. Gen. 38 10361

(http://iopscience.iop.org/0305-4470/38/48/008)

INSTITUTE OF PHYSICS PUBLISHING JOURNAL OF PHYSICS A: MATHEMATICAL AND GENERAL

J. Phys. A: Math. Gen. **38** (2005) 10361–10375 doi:10.1088/0305-4470/38/48/008

# Some novel nonlinear coherent excitations of the Davey–Stewartson system

**X Y Tang**[1], **K W Chow**[2] **and S Y Lou**[1,3]

[1] Department of Physics, Shanghai Jiao Tong University, Shanghai, 200030, People's Republic of China
[2] Department of Mechanical Engineering, University of Hong Kong, Pokfulam Road, Hong Kong
[3] Department of Physics, Ningbo University, Ningbo, 315211, People's Republic of China

Received 13 May 2005, in final form 6 September 2005
Published 16 November 2005
Online at stacks.iop.org/JPhysA/38/10361

**Abstract**
Exact solutions of many integrable (2 + 1) (2 spatial and 1 temporal) dimensional systems of nonlinear evolution equations, e.g., the Davey–Stewartson model, can be obtained by a special separation of variables procedure. By choosing the Jacobi elliptic functions as the building blocks, exact, doubly periodic solutions are obtained analytically. Here, two sets of elliptic functions with two different, independent moduli are employed, and the resulting wave packets are expressed as rational functions of elliptic functions. By taking the long wave limit in one spatial variable, peculiar wave patterns localized in one direction, but periodic in the other direction, will arise. By taking the long wave limit in both spatial variables, exponentially localized wave patterns which differ from the known dromions will result. The boundary conditions relating to these localized structures are studied.

PACS numbers: 02.30.Ik, 02.30.Jr, 47.35.+i

## 1. Introduction

The dynamics of localized structures is a fascinating and important subject in nonlinear science. Many varieties of exotic, one-dimensional localized excitations, e.g., kinks, breathers, instantons, peakons, have been studied earlier in the literature. Similar studies for evolution systems in higher spatial dimensions have been comparatively less numerous. A novel kind of localized structures in integrable (2 + 1) (2 spatial and 1 temporal) dimensional systems of nonlinear evolution equations (NEEs), e.g., the Davey–Stewartson model (DS), was discovered about 20 years ago [1–4]. Such 'dromions' are exponentially localized, and the boundary conditions play a critical role in their dynamics. Discoveries and understanding for (2 + 1)-dimensional NEEs have in general advanced at a tremendous pace in the last decade [5–7].

In one spatial dimension, a periodic wave can usually be regarded as a superposition of an infinite array of equally spaced, identical solitons [8]. The corresponding situation for NEEs in higher spatial dimensions is much less well understood. Though some types of doubly periodic solutions have been obtained [9], the analysis on the components has either not been performed or not completed yet. In some special cases, these doubly periodic patterns can be regarded as the generalization of a two-solitoff, a singly periodic perturbed line soliton or a single straight line kink soliton [10]. Since the dromion is the fundamental coherent structure in $(2 + 1)$ dimensions, it would be natural to investigate if doubly periodic wave patterns can be regarded as a two-dimensional superposition of arrays of dromions.

The boundary conditions play a critical role in the dynamics, as the dromion is situated at the intersection of, or 'driven' by, two line solitons of the corresponding 'mean flow'. In the present work, we are going to present exponentially localized solutions for the DS system. The boundary conditions associated with these special wave patterns will be investigated accordingly.

The DS system is chosen as an illustrative example here for several reasons. Firstly, the dromion was first studied intensively through this system. Secondly, a special procedure, termed here as the multi-linear variable separation approach (MLVSA) [6, 11], was recently established and will give exact solutions for a large number of $(2 + 1)$-dimensional NEEs, including DS. By choosing elementary functions as the building blocks in this algorithm, various localized solutions can be found. In the present approach, the classical Jacobi elliptic functions will be employed as the building blocks, resulting in doubly periodic wave patterns for DS.

The DS equation is an isotropic Lax integrable extension of the well-known $(1 + 1)$-dimensional nonlinear Schrödinger equation and is given as

$$\mathrm{i}u_t + \tfrac{1}{2}(u_{\xi\xi} + u_{\eta\eta}) + \alpha|u|^2u - uv = 0, \qquad v_{\xi\xi} - v_{\eta\eta} - 2\alpha(|u|^2)_{\xi\xi} = 0. \quad (1)$$

From the perspective of fluid dynamics, the DS system can be viewed as the shallow water limit of the Benney–Roskes equation [12, 13], where $u$ is the amplitude of a surface wave packet and $v$ characterizes the mean flow generated by this surface wave. Besides, (1) can also be derived from plasma physics [14], the self-dual Yang–Mills field [15] and quantum field theory [16–18].

A comparison regarding the present approach of MLVSA and those earlier in the literature is in order. The dromion can be derived by Bäcklund transformation [1], inverse scattering type techniques [2, 3] or the Hirota bilinear transformation [4]. For simplicity in the present discussion, we restrict the attention to these three methods, but similar remarks should be applicable to other approaches. In the Bäcklund transformation, a nonlinear superposition formula is employed to compute a structure involving two localized modes, and the phase shifts after interaction are studied accordingly [1]. In the scattering approach, one first transforms the equation using characteristic coordinates. By manipulation of the boundary conditions, energy from the mean flow can be transferred to the wave packet, thus creating focusing effects [2, 3]. Scattering data and the associated integral equations can then be used to construct multi-dromion structures [2, 3]. In the Hirota bilinear approach, special solutions which satisfy the mean flow bilinear equation identically are computed. Such 'ghost solitons' will provide the tracks where the dromion can move [4]. The bilinear equation for the wave packet then determines the structure of the exponentially localized solitary wave.

The present paper employs the multi-linear variable separation approach. One again starts with the DS in characteristic coordinates and then uses a special separation of variables procedure to obtain new solutions. Details have been given in earlier papers [5–7], but a brief sketch is given in the next section. Section 3 deals with the nonlinear coherent structures of the DS system starting from the MLVSA. Doubly periodic (periodic in both directions), semi-localized (decaying in one direction and periodic in the other) and localized (decaying in all directions) structures will be investigated. The last section consists of a short summary and discussion.

## 2. Review of the multi-linear variable separation solution

We first consider the transformation

$$v = p_0(X,t) + q_0(Y,t) - f^{-1}(f_{XX} + f_{YY} + 2f_{XY}) + f^{-2}\big(f_X^2 + 2f_Y f_X + f_Y^2\big), \qquad u = gf^{-1}$$

with $f$ real, $g$ complex, $X = (\xi + \eta)/\sqrt{2}$, $Y = (\xi - \eta)/\sqrt{2}$ and $p_0(X,t) + q_0(Y,t)$ being an arbitrary seed solution of the model. We search for solution of (1) in the form

$$f = a_0 + a_1 p + a_2 q + a_3 pq, \qquad g = p_1 q_1 \exp(\mathrm{i}r + \mathrm{i}s),$$

where $a_0, a_1, a_2, a_3$ are arbitrary constants and $p \equiv p(X,t)$, $q \equiv q(Y,t)$, $p_1 \equiv p_1(X,t)$, $q_1 \equiv q_1(Y,t)$, $r \equiv r(X,t)$, $s \equiv s(Y,t)$ are all real functions of the indicated variables. The exact multi-linear variable separation solution of (1) is derived in the form

$$u = \frac{\sqrt{-2\Delta\alpha^{-1} p_X q_Y}\exp(\mathrm{i}r + \mathrm{i}s)}{a_0 + a_1 p + a_2 q + a_3 pq},$$

$$v = p_0 + q_0 - \frac{(a_2 + a_3 p)q_{YY} + (a_1 + a_3 q)p_{XX}}{a_0 + a_1 p + a_2 q + a_3 pq} + \frac{(a_2 + a_3 p)^2 q_Y^2 - 2\Delta q_Y p_X + (a_1 + a_3 q)^2 p_X^2}{(a_0 + a_1 p + a_2 q + a_3 pq)^2},$$

where

$$p_0 = -\tfrac{1}{8} p_X^{-2}\big(p_{XX}^2 - 2p_X p_{XXX} + c_5 p_X^2\big) - \tfrac{1}{2} r_X^2 - r_t,$$

$$q_0 = -\tfrac{1}{8} q_Y^{-2}\big(q_{YY}^2 - 2q_Y q_{YYY} - c_5 q_Y^2\big) - \tfrac{1}{2} s_Y^2 - s_t,$$

$r$ and $s$ are fixed by

$$p_t = -r_X p_X + c_2(a_2 + a_3 p)^2 + c_3(a_2 + a_3 p) - \Delta c_4,$$

$$q_t = -s_Y q_Y - c_4(a_1 + a_3 q)^2 - c_3(a_1 + a_3 q) + \Delta c_2,$$

$p$ and $q$ are two arbitrary functions, $\Delta \equiv a_0 a_3 - a_1 a_2$, with a constraint $\alpha\Delta p_X q_Y < 0$. In our earlier works, many nonlinear localized excitations, such as multi-dromions, breathers, ring soliton solutions, instantons, have been computed. In addition, some low-dimensional chaotic and fractal patterns including chaotic and fractal dromions have been given. Furthermore, multi-valued solitons called foldons have also been constructed [7].

In this paper, we focus the attention on a special type of travelling waves, $p = P(x) \equiv P(X - v_1 t)$, $q = Q(y) \equiv Q(Y - v_2 t)$, $r = R(x)$, $s = S(y)$ and

$$u = \frac{\sqrt{-2\Delta\alpha^{-1} P_x Q_y}\exp(\mathrm{i}R + \mathrm{i}S)}{a_0 + a_1 P + a_2 Q + a_3 PQ}, \qquad (x = X - v_1 t,\ y = Y - v_2 t), \tag{2}$$

$$v = P_0 + Q_0 - \frac{(a_2 + a_3 P)Q_{yy} + (a_1 + a_3 Q)P_{xx}}{a_0 + a_1 P + a_2 Q + a_3 PQ} + \frac{(a_2 + a_3 P)^2 Q_y^2 - 2\Delta Q_y P_x + (a_1 + a_3 Q)^2 P_x^2}{(a_0 + a_1 P + a_2 Q + a_3 PQ)^2}, \tag{3}$$

with

$$\alpha\Delta P_x Q_y < 0, \tag{4}$$

where $P$, $Q$ are arbitrary functions and

$$P_0 = \frac{P_{xxx}}{4P_x} - \frac{P_{xx}^2}{8P_x^2} - \frac{1}{2}R_x^2 + v_1 R_x - \frac{c_5}{8}, \tag{5}$$

$$Q_0 = \frac{Q_{yyy}}{4Q_y} - \frac{Q_{yy}^2}{8Q_y^2} - \frac{1}{2}S_y^2 + v_2 S_y + \frac{c_5}{8}, \tag{6}$$

$$R_x = v_1 + P_x^{-1}[c_2(a_2 + a_3 P)^2 + c_3(a_2 + a_3 P) - \Delta c_4], \tag{7}$$

$$S_y = v_2 - Q_y^{-1}[c_4(a_1 + a_3 Q)^2 + c_3(a_1 + a_3 Q) - \Delta c_2]. \tag{8}$$

Anticipating that exponentially localized structures will be derived in the subsequent section, it is instructive to derive the simple, localized 1-dromion of (1), using one of the known methods [1–4]. For convenience, we shall choose the bilinear approach where (1) is rewritten as

$$\left[\mathrm{i}D_t + \frac{1}{2}\left(D_\xi^2 + D_\eta^2\right)\right] G \cdot F = 0, \qquad \left(D_\xi^2 - D_\eta^2\right) F \cdot F = 2\alpha G G^*,$$

$$u = \frac{G}{F}, \qquad v = (2\log F)_{\xi\xi},$$

where as usual $D$ is the Hirota operator [4]. The ghost solitons and dromion are computed from the auxiliary functions

$$\begin{aligned} F &= 1 + \exp(\eta_1 + \eta_1^*) + \exp(\eta_2 + \eta_2^*) + M \exp(\eta_1 + \eta_1^* + \eta_2 + \eta_2^*), \\ G &= A_0 \exp(\eta_1 + \eta_2), \qquad \eta_n = \delta_{1n} x + \delta_{2n} y + \Omega_n t, \end{aligned} \tag{9}$$

where $X$ and $Y$ are defined at the beginning of this section. The various parameters in the above equations are chosen to satisfy the bilinear equations [9].

It is then clear that the intensity, or $|G/F|^2$, will typically involve the hyperbolic secant function upon rewriting. Typical new localized solutions derived in this work will involve a combination of the hyperbolic and the inverse trigonometric functions (an example is equation (14) in the next section). Hence, periodic and localized solutions obtained in this work must be different from the known dromions.

## 3. Nonlinear coherent structures

Two criteria will guide our choice of elliptic functions used in the present work. The first one is the constraint $\alpha\Delta P_x Q_y < 0$. The second is that $P$, $Q$ should be expressed in closed forms, without resort to elliptic integrals of the third kind or other even more complicated functions. By choosing elliptic functions with different, independent moduli for $P$, $Q$, doubly periodic patterns of DS are obtained. By choosing one (or both) modulus (moduli) to be one, semi-localized (localized) patterns will result. Furthermore, the boundary conditions in the far field for the mean flow will be addressed, as they will determine if a Hamiltonian will exist in the present case.

### *3.1. First type*

In this case, the two arbitrary functions $P$ and $Q$ are chosen as

$$P = \rho^{-1} \arcsin(\mathrm{sn}(\rho x, k)), \qquad Q = \beta^{-1} \arcsin(\mathrm{sn}(\beta y, k_1)), \tag{10}$$

where $\rho$, $\beta$ are arbitrary constants, $k$, $k_1$ are moduli of the Jacobi elliptic functions which satisfy $P_x = \mathrm{dn}(\rho x, k)$, $Q_y = \mathrm{dn}(\beta y, k_1)$. The constraint (4) can be satisfied as dn is always

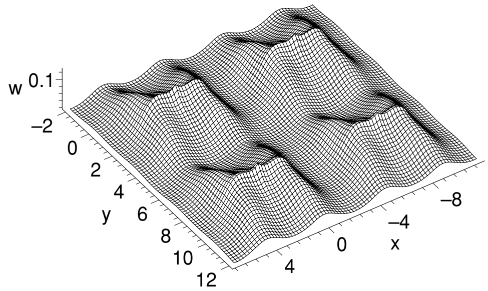


**Figure 1.** Structure of the intensity $w \equiv |u|^2$ (11) with $a_0 = 8, a_1 = a_2 = -1, a_3 = -0.5, \alpha = 2, \rho = \beta = 1, k = 0.9, k_1 = 0.6$.

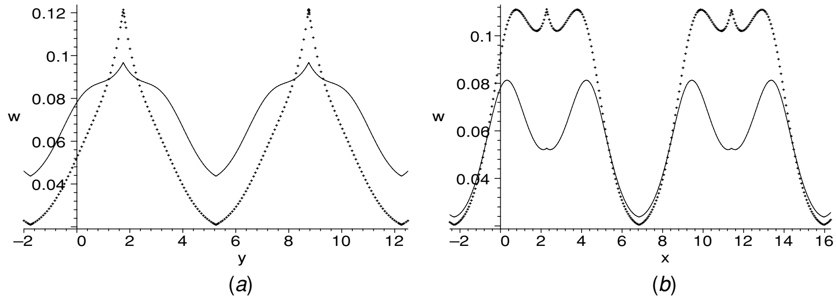


**Figure 2.** Plot of $w$ (11) with constants same as those in figure 1 along the directions ($a$) $x = 2$ (point) and $x = 0$ (solid); ($b$) $y = 2$ (point) and $y = 0$ (solid).

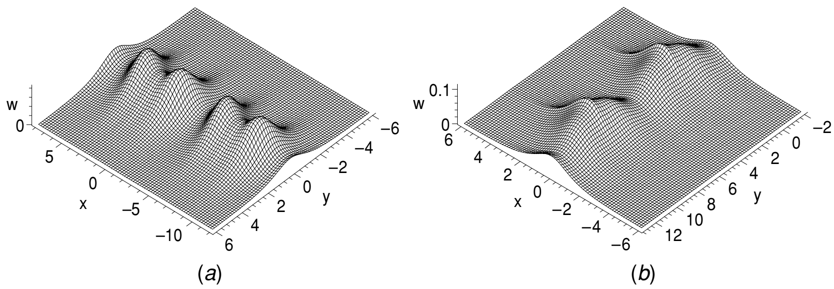


**Figure 3.** Semi-localized structure of $w$ (11) for ($a$) $k = 0.9, k_1 = 1$; ($b$) $k = 1, k_1 = 0.6$, with other constants same as those in figure 1.

positive and the product of $\alpha$ and $\Delta$ can be negative. The formulations (2)–(8), (10) will give the multi-linear variable separation solution of DS. In general, the wave packet $u$ will exhibit a doubly periodic pattern (figure 1). For typical values of the parameters, the number of peaks, or local maxima, in the $x$ and $y$ directions might be different (figure 2). The intensity $w$ ($w \equiv |u|^2$) is given by

$$w = -2\Delta\alpha^{-1}\beta^2\rho^2 \,\mathrm{dn}(\rho x, k)\,\mathrm{dn}(\beta y, k_1)[a_0\beta\rho + a_1\beta \arcsin(\mathrm{sn}(\rho x, k)) + a_2\rho \arcsin(\mathrm{sn}(\beta y, k_1)) + a_3 \arcsin(\mathrm{sn}(\rho x, k)) \arcsin(\mathrm{sn}(\beta y, k_1))]^{-2}. \tag{11}$$

By taking one of the moduli to be unity, patterns periodic in one direction but localized in the other are obtained. Figures 3($a$) and ($b$) illustrate this scenario. The remarkable case

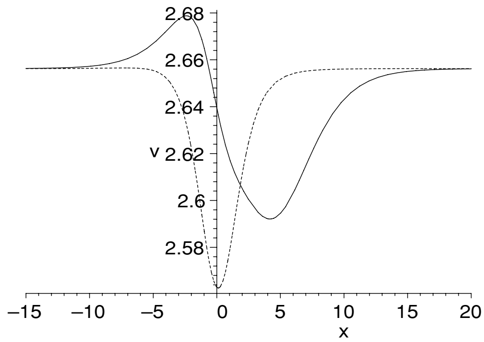


**Figure 4.** Asymptotic behaviours of the mean flow $v$ of the first type, with $k = k_1 = v_1 = 1$, $v_2 = 2$, $\rho = 0.5$ and others are same as those in figure 1, dotted line is for $y \to -\infty$ and solid line for $y \to +\infty$.

occurs when both moduli are allowed to tend to 1, formulations (2)–(8), (10) then yield the exponentially localized structure

$$w \equiv |u|^2 = -2\Delta\alpha^{-1}\beta^2\rho^2 \mathrm{sech}(\rho x)\mathrm{sech}(\beta y)[a_0\beta\rho + a_1\beta \arcsin(\tanh(\rho x)) + a_2\rho \arcsin(\tanh(\beta y)) + a_3 \arcsin(\tanh(\rho x)) \arcsin(\tanh(\beta y))]^{-2}. \quad (12)$$

One can then conclude that this expression is a dromion, defined here loosely as an exponentially localized solution. However, (12) is different from a known, conventional dromion [1–4] given in (9), which is typically given entirely in terms of exponential functions only.

An additional feature which reassures this distinction is that many of our new solutions (first to fourth types) here exhibit discontinuities in derivatives or jumps due to the following reason. Given the derivative of an elliptic function,

$$\frac{\mathrm{d}}{\mathrm{d}x}\,\mathrm{sn}(x) = \mathrm{cn}(x)\,\mathrm{dn}(x),$$

we deduce that

$$\int \mathrm{dn}(x)\,\mathrm{d}x = \sin^{-1}(\mathrm{sn}(x)),$$

and we insist that the inverse sine function must be taken from the interval $\left(-\frac{\pi}{2}, \frac{\pi}{2}\right)$. Indeed wave profiles with jumps have been studied rather intensively for one-dimensional evolution equations [19–23]. What we have demonstrated here is that such wave patterns with jumps in derivatives also occur in two or higher spatial dimensions.

The existence of the Hamiltonian of the DS equation is related to the boundary conditions in the far field. The Hamiltonian cannot be constructed unless the cross sections of $v$ at $x = +\infty$ and $y = +\infty$ coincide with those at $x = -\infty$ and $y = -\infty$, respectively [24, 25].

Due to the analytical complexity of $v$, only the pictures related to the asymptotic behaviour of the mean flow under the long wave limit are explicitly depicted. To obtain non-singular solutions, the arbitrary constants $c_2$, $c_3$ and $c_4$ must be zero. Figure 4 shows that the mean flow has different asymptotic behaviours for $y \to +\infty$ and $y \to -\infty$ in the domain around $x = 0$. Hence, the Hamiltonian does not exist in this case.

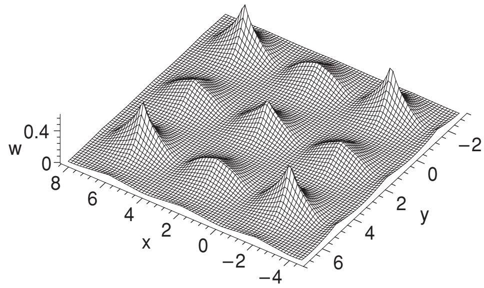


**Figure 5.** Structure of the intensity $w \equiv |u|^2$ (14) with $\alpha = 2, \beta = \rho = -a_3 = 1, a_0 = 10, a_1 = a_2 = \frac{1}{3}, k = 0.8, k_1 = 0.3$.

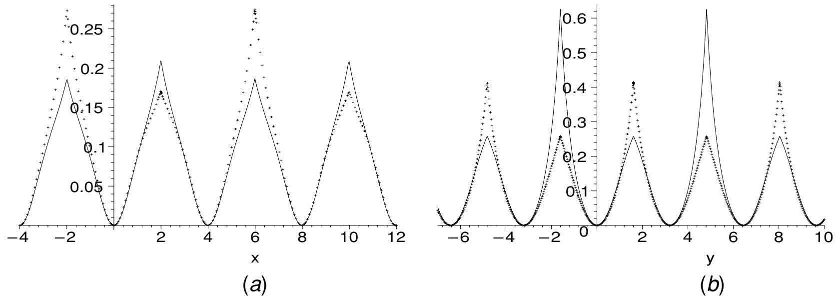


**Figure 6.** Plot of $w$ (14) with same constants as those in figure 5 along (*a*) $y = -2$ (point) and $y = 2$ (solid); (*b*) $x = 2$ (point) and $x = -2$ (solid).

### *3.2. Second type*

Secondly, we choose $P$ and $Q$ as

$$P = (3\rho)^{-1}[\arcsin(\mathrm{sn}(\rho x, k))]^3, \qquad Q = (3\beta)^{-1}[\arcsin(\mathrm{sn}(\beta y, k_1))]^3, \tag{13}$$

so that $P_x = [\arcsin(\mathrm{sn}(\rho x, k))]^2\,\mathrm{dn}(\rho x, k)$, $Q_y = [\arcsin(\mathrm{sn}(\beta y, k_1))]^2\,\mathrm{dn}(\beta y, k_1)$. The intensity $w$ ($w \equiv |u|^2$) is (figure 5)

$$\begin{aligned} w = {} & -162\Delta\alpha^{-1}\beta^2\rho^2\,\mathrm{dn}(\rho x, k)\,\mathrm{dn}(\beta y, k_1)[\arcsin(\mathrm{sn}(\rho x, k))]^2[\arcsin(\mathrm{sn}(\beta y, k_1))]^2 \\ & \times [9a_0\beta\rho + 3a_1\beta[\arcsin(\mathrm{sn}(\rho x, k))]^3 + 3a_2\rho[\arcsin(\mathrm{sn}(\beta y, k_1))]^3 \\ & + a_3[\arcsin(\mathrm{sn}(\rho x, k))]^3[\arcsin(\mathrm{sn}(\beta y, k_1))]^3]^{-2}. \end{aligned} \tag{14}$$

Rather novel patterns can be seen from the cross-sectional pictures. For a cross section in $y$ there are two peaks with different amplitudes in one period (figure 6(*a*)), and the same is true for a cross section in $x$ (figure 6(*b*)).

Similarly, the long wave limits of (14) are also instructive. Here, we fix $k = 1, k_1 = 0.1$ (or $k_1 = 1, k = 0.5$), the pattern is localized in the $x$ (or $y$) direction but periodic in $y$ (or $x$), with four peaks per period (figure 7(*a*) (or (*b*))). With $k_1$ and $k$ tending to one simultaneously, a novel dromion with four non-identical peaks separated by two perpendicular narrow gaps appears (figure 8). This is not a 4-dromion structure, as a conventional 4-dromion has four underlying path lines, and the four dromions are located at the intersections of these lines. The dromion here (figure 8) is driven by two perpendicular lines.

The precise expression for the mean flow field $v$ can be readily deduced by substituting (5)–(8) and (13) into (3). To avoid singular solutions, the constants $c_2, c_3, c_4$ again have to

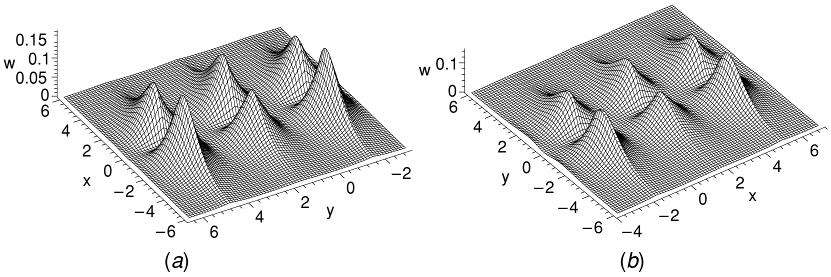


**Figure 7.** Semi-localized structure of $w$ (14) for ($a$) $k = 1, k_1 = 0.1$; ($b$) $k = 0.5, k_1 = 1$, with other constants same as those in figure 5.

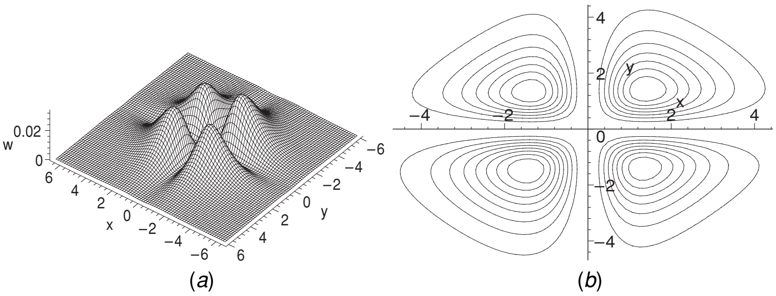


**Figure 8.** ($a$) Localized structure of $w$ (14) for $k = k_1 = 1$, other constants are the same as those in figure 5. ($b$) Contour plot of ($a$).

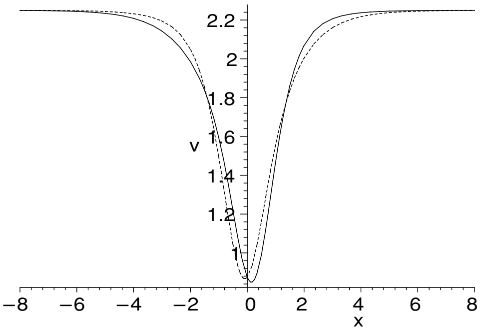


**Figure 9.** Asymptotic behaviours of the mean flow $v$ of the second type, with $k = k_1$, $v_1 = 2$, $v_2 = 0$ and others are same as those in figure 5, dotted line is for $y \to -\infty$ and solid line for $y \to +\infty$.

be zero. For a typical set of parameters, a plot of the mean flow in the far field again shows different asymptotic behaviour, and hence a Hamiltonian also does not exist in this case.

The interactions of dromions deserve further investigations. The interactions can be elastic (identities retained except possibly for phase shifts) or inelastic (with shapes exchanged entirely or partially). Fusion or fission of component solitons has also been observed in such interaction processes. In order to study the interaction property of the new dromion solution shown in figure 8, we first write down the expression for a 2-dromion solution in the original

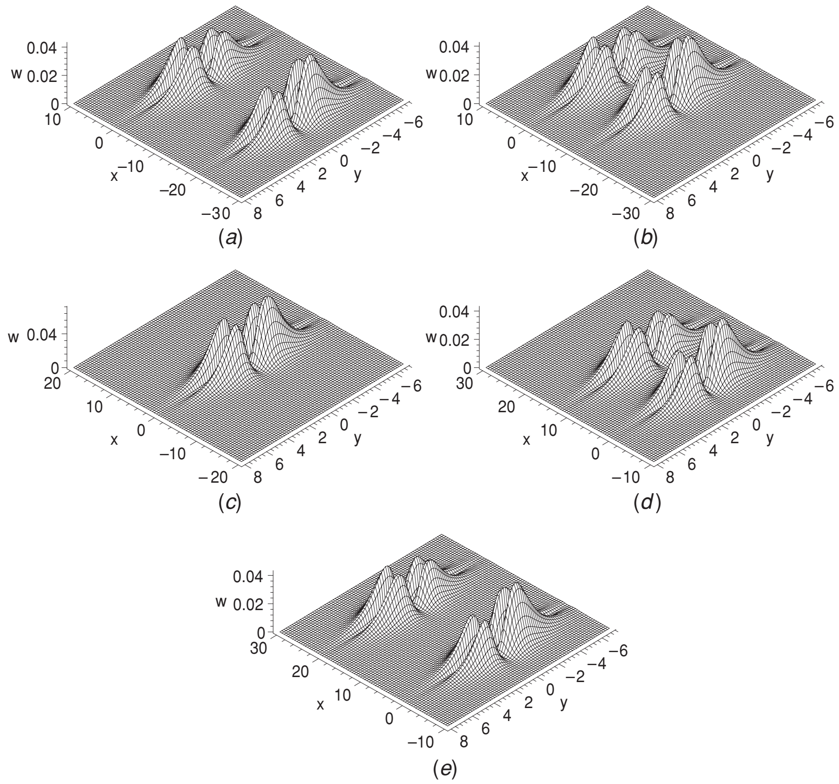


**Figure 10.** Interactions between two dromions expressed by (15) with (16), (17) and $\alpha = 2$, $\beta = \rho = \rho_1 = -a_3 = 1$, $a_0 = 10$, $a_1 = a_2 = \frac{1}{3}$, $v_1 = 4$, $v_2 = v_3 = 0$ at times (*a*) $t = -5$, (*b*) $t = -3$, (*c*) $t = 0$, (*d*) $t = 3$ and (*e*) $t = 5$.

coordinates,

$$w \equiv |u|^2 = \frac{-2\Delta\alpha^{-1} p_x q_y}{(a_0 + a_1 p + a_2 q + a_3 pq)^2}, \tag{15}$$

with

$$p = \frac{\arcsin(\tanh(\rho(x - v_1 t)))^3}{3\rho} + \frac{\arcsin(\tanh(\rho_1(x - v_3 t)))^3}{3\rho_1}, \tag{16}$$

$$q = \frac{\arcsin(\tanh(\beta(y - v_2 t)))^3}{3\beta}. \tag{17}$$

We set one of the two dromions to move along the $x$-axis with the velocity $v_1 = 4$ and the other as static or $v_2 = v_3 = 0$. Figure 10 shows the collision of two dromions. Initially ($t = -5$), the dromion located at the point $(0, 0)$ is stationary and the other located at the point $(-20, 0)$ is moving towards the static one (figure 10(*a*) and (*b*)). At $t = 0$, they merge to form a single entity (figure 10(*c*)) and then separate (figure 10(*d*) and (*e*)). Eventually, at time $t = 5$, the moving one reaches the point $(20, 0)$ and the static one is still at $(0, 0)$. We can either regard this interaction process as one where the two dromions totally exchange their shapes with their velocities preserved. Alternatively, we can regard the initially moving

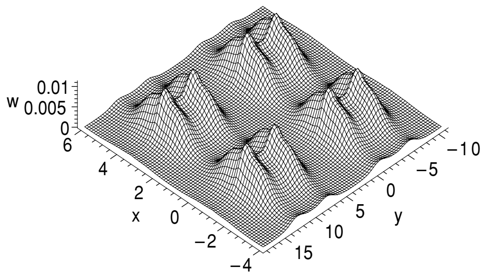

**Figure 11.** Structure of $w$ (19) with $a_0 = 6, a_1 = -a_3 = \beta = 1, a_2 = \rho = \alpha = 2, k = 0.9, k_1 = 0.99$.

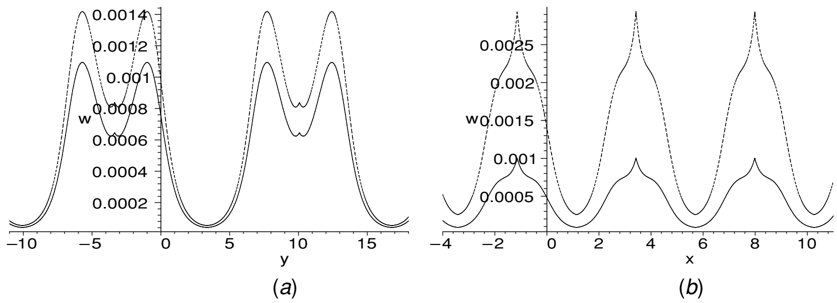

**Figure 12.** The section structure of figure 9 for (*a*) $x = 1$ (solid) and $x = 1.5$ (dotted); (*b*) $y = 1$ (dotted) and $y = 2$ (solid).

soliton has been reduced to stationary after the collision and the momentum has been totally transferred to the dromion moving at the later time. Either way, the interaction between these two dromions is inelastic.

### *3.3. Third type*

$P$ and $Q$ are now assumed to be

$$P = -[\rho(3 + \arcsin(\mathrm{sn}(\rho x, k)))]^{-1}, \qquad Q = -[\beta(3 + \arcsin(\mathrm{sn}(\beta y, k_1)))]^{-1}, \tag{18}$$

such that $P_x = \mathrm{dn}(\rho x, k)[3+\arcsin(\mathrm{sn}(\rho x, k))]^{-2}$, $Q_y = \mathrm{dn}(\beta y, k_1)[3+\arcsin(\mathrm{sn}(\beta y, k_1))]^{-2}$. Therefore, (2) becomes ($w \equiv |u|^2$)

$$w = -2\Delta\alpha^{-1}\beta^2\rho^2\,\mathrm{dn}(\rho x, k)\,\mathrm{sn}(\beta y, k_1)\{a_0\beta\rho[3 + \arcsin(\mathrm{sn}(\rho x, k))][3 + \arcsin(\mathrm{sn}(\beta y, k_1))] - a_1\beta[3 + \arcsin(\mathrm{sn}(\beta y, k_1))] - a_2\rho[3 + \arcsin(\mathrm{sn}(\rho x, k))] + a_3\}^{-2}. \tag{19}$$

The pattern is generally still doubly periodic (figure 11). For typical parameter values, there might be two symmetric apexes for a cross section in $x$ (figure 12(*a*)). For a cross section in $y$, there might be corner-like structures (figure 12(*b*)), where the derivatives will be discontinuous.

Figure 13(*a*) shows the semi-localized structure ($k_1$ being 1 while $0 < k < 1$). Figure 13(*b*) shows the opposite limit of $k$ being 1 while $0 < k_1 < 1$. Both structures are periodic in one direction, but localized in the other. Figure 14 illustrates another exponentially localized structure (both $k_1$ and $k$ being 1).

To obtain a non-singular asymptotic solution for the mean flow $v$, the arbitrary constants $c_2, c_3$ and $c_4$ must again be zero. Figure 15(*a*), plotted for the mean flow of this type at

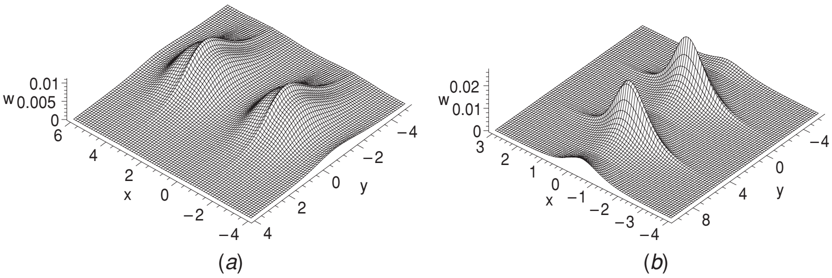


**Figure 13.** The semi-localized structures of $w$ (19) for (*a*) $k = 0.9, k_1 = 1$; (*b*) $k = 1, k_1 = 0.3$, other constants are same as those in figure 11.

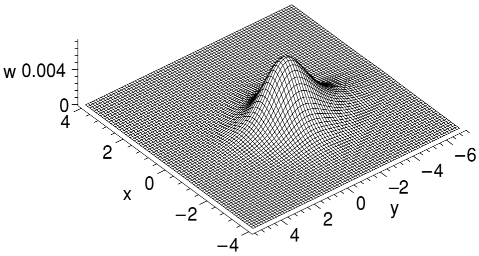


**Figure 14.** The localized structure of $w$ (19) with $k = k_1 = 1$ and other constants same as those in figure 11.

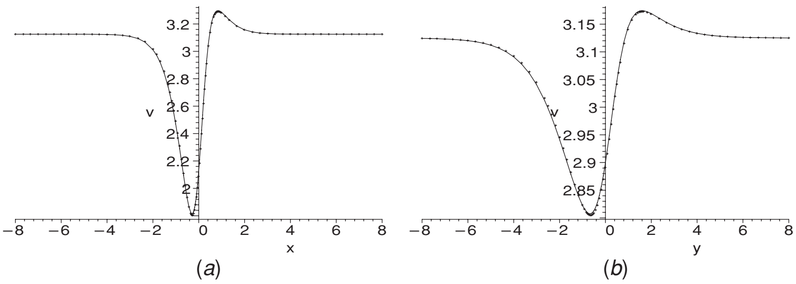


**Figure 15.** Asymptotic behaviours of the mean flow $v$ of the third type, with $k = k_1 = v_1 = 1, v_2 = 2$ and other constants same as those in figure 11: (*a*) dotted line for $y \to +\infty$ and solid line for $y \to -\infty$; (*b*) dotted line for $x \to +\infty$ and solid line for $x \to -\infty$.

$y \to +\infty$ (dotted line) and $y \to -\infty$ (solid line), reveals the same asymptotic behaviours of $v$ when $y \to \pm\infty$. This result is different from those of the first and second types. The same asymptotic behaviours of $v$ when $x \to \pm\infty$ are plotted in figure 15(*b*). Consequently, the condition for a Hamiltonian to exist [24, 25] is satisfied. Further, the mean flow has the same value for $x \to \pm\infty$, $y \to \pm\infty$, that is, $v|_{x\to\pm\infty, y\to\pm\infty} = \frac{25}{8}$.

### *3.4. Fourth type*

Finally, $P$ and $Q$ are chosen as

$$
\begin{aligned}
P &= \frac{1}{2\rho}[(2 - k^2)\arcsin(\mathrm{sn}(\rho x, k)) + k^2\,\mathrm{sn}(\rho x, k)\,\mathrm{cn}(\rho x, k)], \\
Q &= \frac{1}{2\beta}\left[\left(2 - k_1^2\right)\arcsin(\mathrm{sn}(\beta y, k_1)) + k_1^2\,\mathrm{sn}(\beta y, k_1)\,\mathrm{cn}(\beta y, k_1)\right],
\end{aligned}
\tag{20}
$$

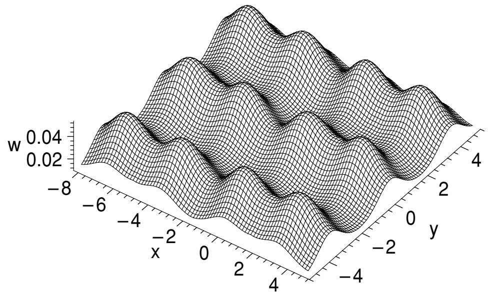


**Figure 16.** Plot of $w$ (21) with (22) and $k = 0.5$, $k_1 = 0.7$.

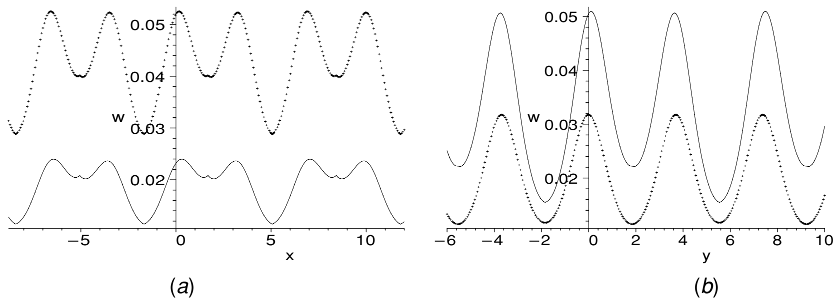


**Figure 17.** Some section structure related to figure 16 along ($a$) $y = 0.2$ (solid line) and $y = 1.5$ (dotted line); ($b$) $x = 0.5$ (solid line) and $x = -2$ (dotted line), respectively.

such that $P_x = \mathrm{dn}(\rho x, k)^3$, $Q_y = \mathrm{dn}(\beta y, k_1)^3$. Substituting (20) into (2) will yield an expression for the intensity ($w \equiv |u|^2$)

$$\begin{aligned} w = {} & -32\Delta\alpha^{-1}\beta^2\rho^2\,\mathrm{dn}(\rho x, k)^3\,\mathrm{dn}(\beta y, k_1)^3\big\{4a_0\beta\rho + 2a_1\beta\big[\big(2-k_1^2\big)\arcsin(\mathrm{sn}(\beta y, k_1)) \\ & + k_1^2\,\mathrm{sn}(\beta y, k_1)\,\mathrm{cn}(\beta y, k_1)\big] + 2a_2\rho[(2-k^2)\arcsin(\mathrm{sn}(\rho x, k)) \\ & + k^2\,\mathrm{sn}(\rho x, k)\,\mathrm{cn}(\rho x, k)] + a_3\big[\big(2-k_1^2\big)\arcsin(\mathrm{sn}(\beta y, k_1)) \\ & + k_1^2\,\mathrm{sn}(\beta y, k_1)\,\mathrm{cn}(\beta y, k_1)\big][(2-k^2)\arcsin(\mathrm{sn}(\rho x, k)) \\ & + k^2\,\mathrm{sn}(\rho x, k)\,\mathrm{cn}(\rho x, k)]\big\}^{-2}. \end{aligned} \tag{21}$$

Figure 16 illustrates the wave pattern for some typical values of the parameters

$$a_0 = 20, \qquad a_1 = a_2 = a_3 = -1, \qquad \beta = \rho = 1, \qquad \alpha = 2, \tag{22}$$

and $k = 0.5$, $k_1 = 0.7$.

Some cross-sectional structures are shown in figure 17($a$) along $y = 0.2$ (solid line) and $y = 1.5$ (dotted line), and figure 17($b$) along $x = 0.5$ (solid line) and $x = -2$ (dotted line). The wave pattern is thus clearly doubly periodic. When only one of the moduli approaches 1, then a semi-localized structure is generated (figure 18($a$) for $k = 1$ and figure 18($b$) for $k_1 = 1$). Although these two semi-localized structures are different from each other, they degenerate to the same dromion structure if both moduli are 1.

To avoid a singular solution here again forces the constants $c_2$, $c_3$ and $c_4$ to be zero. The asymptotic values of $x$ or $y$ for large values of the arguments in this case are computed to be $19/4$, which is shown in figure 19. Thus, a Hamiltonian might exist in this case.

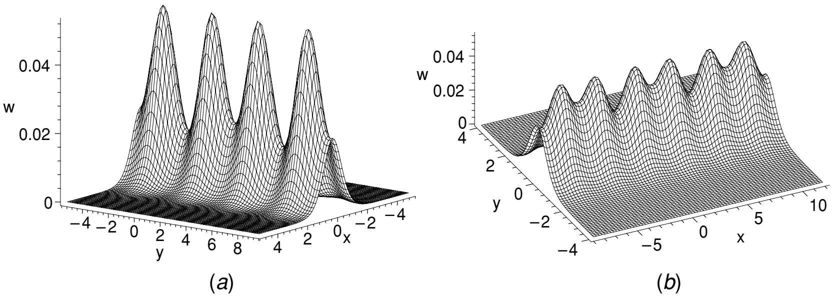


**Figure 18.** Plot of $w$ (21) with (22) under the long wave limit as (*a*) $k = 1, k_1 = 0.7$; (*b*) $k = 0.5, k_1 = 1$, respectively.

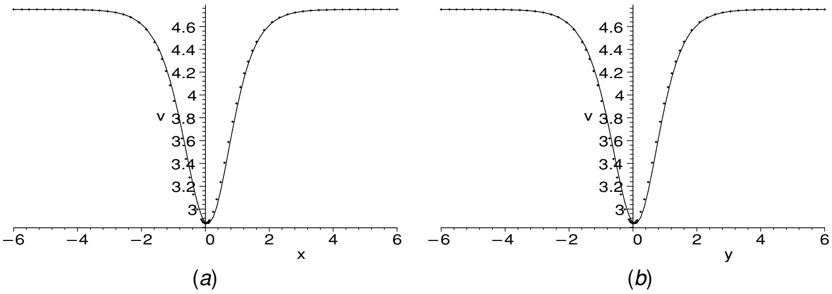


**Figure 19.** Asymptotic behaviours of the mean flow $v$ of the fourth type, with $k = k_1 = v_1 = 1$, $v_2 = 2$ and (22): (*a*) dotted line is for $y \to +\infty$ and solid line for $y \to -\infty$; (*b*) dotted line is for $x \to +\infty$ and solid line for $x \to -\infty$.

## 4. Summary and discussions

A class of doubly periodic solutions of the Davey–Stewartson system has been studied by employing the classical, Jacobi elliptic functions as the building blocks for the multi-linear variable separation solution. For minimal algebraic complexity, attention is restricted to cases where analytical, closed form expressions are obtained. The internal structures of the wave packet, in terms of say the number of local maxima and minima, will depend on the choice of elliptic functions and also on the two distinct, independent moduli. A semi-localized pattern, namely one which is periodic in one direction, but localized in the other, can be obtained by choosing one of the moduli to be unity.

The boundary condition is investigated from two perspectives, one as the driving force behind the dromion, the other as to the existence of a Hamiltonian.

New exponentially localized units, or dromions, will result if both moduli are tending to 1 as a limit. They are different from the conventional expressions and we believe that they deserve further study. In fact some of new localized units discussed in this paper have four distinct peaks, but they are not 4-dromion, as their underlying structures of the wave packet are different. The interaction between two dromions of this type is studied. One interpretation shows that they preserve their velocities, but totally exchange their shapes without phase shifts during the interaction.

Many aspects of the present approach remain incomplete, and further studies will definitely reveal new solutions and new surprises. One problem which we only briefly touch upon in this paper is the collisions of dromions. Similar to the issue of their derivation, collisions of these exponentially localized units can be studied by a variety of methods. Employing scattering techniques, earlier works have shown that dromions in general do not retain their forms upon interaction, though special regimes of parameters can be selected when shapes do remain preserved [3]. A direct approach for the present case of DS system also exists, where phase shift and changes in amplitude can be studied from a matrix formulation. Head-on collisions and scattering of dromions can be investigated and computer plots demonstrate very novel details of the interaction process [26]. Indeed, further works confirm a new class of solutions for DS known as 'solitoffs' or entities decaying exponentially in all directions except a preferred one. Collisions or interactions between a dromion and a solitoff can be expressed analytically [27]. The present work suggests another approach to this problem of dromion interaction, and that is choosing different numbers of modes in this separation of variable approach, and one simple application, namely, collision of dromions with four peaks, is illustrated for the second type of solutions.

Secondly, we have avoided any use of the elliptic integral of the third kind in the present formulation. Whether the inclusion of this larger class of functions will lead to new structures of the wave packet is not known.

## Acknowledgments

The work was supported by the National Natural Science Foundations of China (nos 90203001 and 10475055). Partial financial support for KWC has been provided by the Research Grants Council through contracts HKU 7184/04E and HKU 7123/05E.

## References

[1] Boiti M, Leon J J P, Martina L and Penpinelli F 1988 *Phys. Lett.* A **132** 432
[2] Fokas A S and Santini P M 1989 *Phys. Rev. Lett.* **63** 1329
[3] Fokas A S and Santini P M 1990 *Physica* D **44** 99
[4] Hietarinta J and Hirota R 1990 *Phys. Lett.* A **145** 237
[5] Lou S Y 2000 *Phys. Lett.* A **277** 94
Lou S Y and Ruan H Y 2001 *J. Phys. A: Math. Gen.* **35** 305
[6] Tang X Y, Lou S Y and Zhang Y 2002 *Phys. Rev.* E **66** 046601
[7] Tang X Y and Lou S Y 2003 *J. Math. Phys.* **44** 4000
Tang X Y and Lou S Y 2003 *Commun. Theor. Phys.* **40** 62
[8] Whitham G B 1984 *IMA J. Appl. Math.* **32** 353
Boyd J P 1984 *SIAM J. Appl. Math.* **44** 952
Miloh T 1990 *J. Fluid Mech.* **211** 617
Chow K W 1993 *J. Phys. Soc. Japan* **62** 2007
[9] Chow K W, Ko N W M and Tang S K 1997 *Fluid Dyn. Res.* **21** 101
Chow K W 2002 *Wave Motion* **35** 71
[10] Lou S Y, Hu H C and Tang X Y 2005 *Phys. Rev.* E **71** 036604
[11] Lou S Y and Lu J Z 1996 *J. Phys. A: Math. Gen.* **29** 4209
Qian X M, Lou S Y and Hu X B 2004 *J. Phys. A: Gen. Math.* **37** 2401
[12] Benney D J and Roskes G J 1969 *Stud. Appl. Math.* **47** 377
[13] Davey A and Stewartson K 1974 *Proc. R. Soc.* A **338** 101
[14] Nishinari K, Abe K and Satsuma J 1993 *J. Phys. Soc. Japan* **62** 2021
[15] Ablowitz M J and Clarkson P A 1991 *Solitons, Nonlinear Evolution Equations and Inverse Scattering (London Mathematical Society Lecture Note Series* vol 149*)* (Cambridge: Cambridge University Press)
[16] Schultz C L, Ablowitz M J and BarYaacov D 1987 *Phys. Rev. Lett.* **59** 2825
[17] Kulish P P and Lipovsky V D 1988 *Phys. Lett.* A **127** 413
[18] Pang G D, Pu F C and Zhao B H 1990 *Phys. Rev. Lett.* **65** 3227
[19] Kraenkel R A, Senthilvelan M and Zenchuk A I 2000 *Phys. Lett.* A **273** 183
[20] Qian T and Tang M 2001 *Chaos Solitons Fractals* **12** 1347

[21] Johnson R S 2003 *Proc. R. Soc.* A **459** 1687
[22] Vakhnenko V O and Parkes E J 2004 *Chaos Solitons Fractals* **20** 1059
[23] Bai C L 2004 *J. Phys. Soc. Japan* **73** 37
[24] Nishinari K and Jajima T 1995 *Phys. Rev.* E **51** 4986
[25] Yoshida N, Nishinari K, Satsuma J and Abe K 1998 *J. Phys. A: Math. Gen.* **31** 3325
[26] Gilson C R and Nimmo J J C 1991 *Proc. R. Soc.* A **435** 339
[27] Gilson C R 1992 *Phys. Lett.* A **161** 423